Liquid-Phase Sintering and Properties of PIMed 10-20 vol.% SiC_p-Reinforced Aluminium Composites

Tapany Patcharawit[1,a], Arada Ngeekoh[1], Usanee Kitkhamthorn[1] and Nutthita Chuankrekkul[2]

[1]*School of Metallurgical Engineering, Suranaree University of Technology, 111 University Avenue, Muang, Nakhon Ratchasima, 30000, Thailand*
[2]*The Metallurgy and Materials Science Research Institute, Chulalongkorn University, Phayatai Road, Patumwan, Bangkok, 10330, Thailand*

Abstract. Liquid-phase sintering and properties of powder injection moulded aluminium composite reinforced with SiC_p has been investigated via thermal-phase analyses and hardness property. Mixing of 10 and 20 vol.% SiC_p and aluminium powder was done via ball milling prior to feedstock preparation at 55% solid loading. Powder injection moulding was carried out at 170°C, followed by solvent and thermal debinding. The brown samples were sintered in a nitrogen atmosphere at 650-660°C, prior to age-hardening. Experimental result shows relatively high % linear shrinkage of 9.9-21.9 % and high % volumetric shrinkage of 34.5-46.5%. Thermal analysis indicates the formation of the liquid around 632 °C, facilitating liquid phase sintering. The composite microstructures consists of uniformly distributed SiC_p throughout the densified aluminium matrix. SiC_p addition scales up SiC_p clustering, accompanying with gap porosity. The composite reinforced with 10 vol.% SiC_p possesses higher sintered density at 2.63 g/cm^3, yielding 93.1% theoretical. However the maximum macro Vickers hardness was measured at 164.2 H_v for 20 vol.% SiC_p – reinforced aluminium composite in the age-hardened condition. Liquid phase sintering was found effective for the microstructure evolution of the PIMed composite, rendering densification. Hardening is influenced by SiC_p addition and the roles of AlN, Al_2Cu and Mg_2Si precipitates.

1 Introduction

Aluminium matrix composites have been increasingly recognized for engineering applications such as in the automotive, electronics, aerospace and biomedical fields for examples [1-3]. Their properties are dependent on selected materials utilized such as the matrix alloys and reinforcements. Particulate reinforcement such as Al_2O_3, SiC, Si_3N_4, and AlN are of great interest for improvement of hardness, tensile, modulus and wear properties. Powder injection moulding (PIM) is one of the most effective solid-state fabrication techniques available for composite production in which tailored properties can be achieved by selection of the matrices and reinforcements in the powder mixing stage. The PIM process involves powder pre-treatment, feedstock preparation, injection moulding, followed by debinding, and finally sintering along with post-treatment if required. Particularly in the sintering stage, strength development is due to bonding of adjoining powders via solid/liquid phase sintering. Solid phase sintering at a temperature range just below the melting point of the powder renders strong

[a] Tapany Patcharawit: tapany@sut.ac.th

solid bonds via material transport mechanisms such as lattice diffusion, grain boundary diffusion, viscous flow, surface diffusion, gas phase transport for example [4]. Grain boundary is the most important source of materials for diffusion to take place. However, as the sintering temperature is raised to just above the solidus of the components; hence, some extent of the liquid forms, which contributes to densification and shrinkage. The viscous flow is enhanced favourable for fast sintering. The assisting requirements are 1) increasing solid solubility in the newly formed liquid melt, 2) solubility of solid in the liquid and 3) low liquid solubility in the solid [5]. Additives which lower liquidus and solidus temperatures are also favourable.

As for the PIMed aluminium composites investigated in this current research, the formulated composition involved deformable, lower melting point Al-Cu alloy powder as the matrix and hard-abrasive, high melting point SiC_p of a smaller size as the reinforcement, aiming for hardness and wear improvement. Hardening is expected via second phase precipitation and particulate reinforcement. Liquid phase sintering was applied to improve densification on the expense of shrinkage and dimension stability. The influences of SiC_p addition along with microstructure evolution during liquid phase sintering is also discussed.

2 Experimental

The commercial Al-Cu powder has its composition as detailed in Table 1 and its average size is 73 μm. The silicon carbide particulate (SiC_p) of averagely 20 μm size was added at 10 and 20 vol.%. Feedstocks was prepared at 55 % solid loading for powder injection moulding at 170^{o}C. The obtained green samples of 20x20x5 mm^3 dimensions were subjected to solution debinding. In order to determine the sintering temperature of the composite, Simultaneous Thermal Analysis (STA) was selected using a NETZSCH STA 449 F3 Jupiter operating at a 40 K/min heating rate over 25-900^{o}C in a nitrogen atmosphere. Microstructure and phase analysis were carried out after sintering and age-hardening using a JEOL-JSM 6061LV SEM coupled with EDX spectroscopy, and a D8 XRD over a 2θ range of 20^o-80^o. Bulk density and macro Vickers hardness was examined to relate microstructure and property of the composites.

Table 1. Chemical composition of Al-Cu powder by XRF (wt.%).

Al	Cu	Mg	Si	Fe
Balanced	4.77	1.11	1.01	0.12

3 Experimental Results

3.1 Thermal Analysis and Microstructure Examination

3.1.1 Thermal Analysis of the Composite

Differential Scanning Calorimetry (DSC) and Thermogravimetric (TG) analyses are graphically demonstrated in Figs. 1 a) and b) for green compacts of 10 vol.% and 20 vol.% SiC_p additions respectively. It can be seen that the endothermic reactions observed on the DSC curves occurring over 42-156^{o}C are in accordance with the melting ranges of paraffin wax, stearic acid and polypropylene respectively. Accordingly, the moulding temperature was set at 170^{o}C in order to enable a decent flow of feedstock into the mould cavity. Another endothermic reaction at approximately 458^{o}C is possibly incident for the decomposition or vaporization of polypropylene while the TG curves signify mass losses at the onset of 226 ^{o}C towards 471-483^{o}C. This therefore implies a complete thermal debinding of the multi-component binder around 500^{o}C prior to entering liquid phase sintering. Moreover, at approximately 632^{o}C, endothermic reaction is visible due probably to the liquid phase formation [6].

It is therefore recommended that the sintering temperature should be in a range of 650-660°C to achieve liquid phase sintering for such PIMed composites.

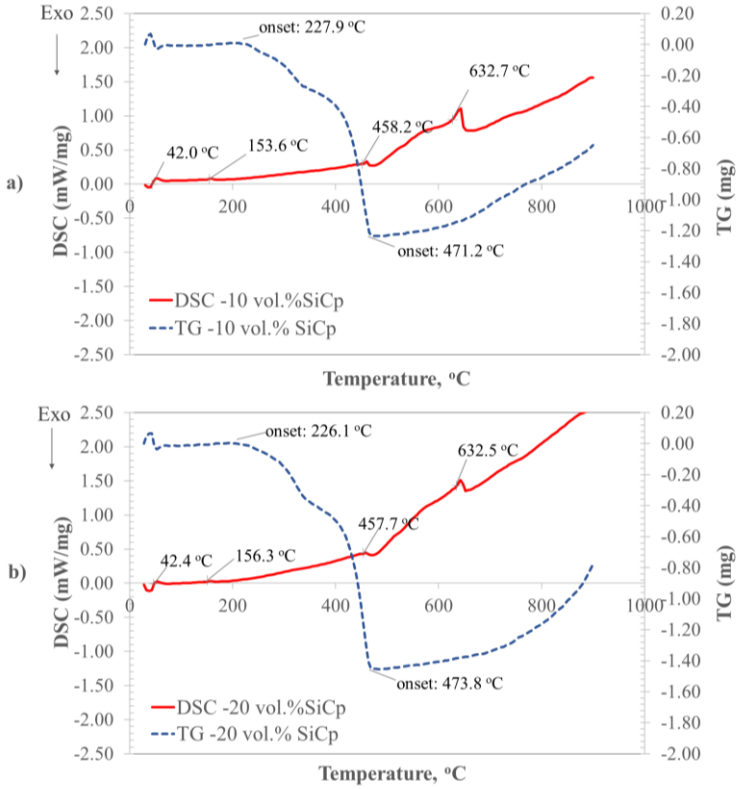

Figure 1. DSC and TG analyses of 10 and 20 vol.% SiC_p green compacts.

3.1.2 Microstructure Analysis

Optical micrographs of 10 and 20 vol.% SiC_p – reinforced aluminium composites in the as-sintered condition are comparatively shown in Figs. 2 a) and b) respectively. Fine SiC_p (dark) is distributed throughout the aluminium matrix (light). There is no excessive grain growth of the matrix. Al-SiC_p interfaces exhibit good bonding. A greater degree of SiC_p agglomeration was observed at higher SiC_p content, giving greater amount of SiC_p-SiC_p interfaces and a higher degree of porosity.

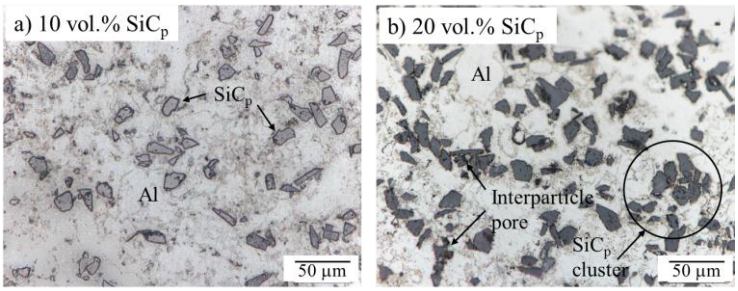

Figure 2. Optical micrographs of 10 and 20 vol.% SiC_p reinforced aluminium composites.

3.1.3 XRD Analysis

XRD results are illustrated in Figs. 3 a) - d) for 10 and 20 vol.% SiC_p – reinforced aluminium composites in the as-sintered and age-hardened conditions. Existence of phases are quite similar for both composites reinforced with 10 and 20 vol.% SiC_p. The main peaks of Al were detected as the matrix. The SiC peaks were also identified as the reinforcement and it is more evidently shown especially for composite possessing higher SiC_p addition. AlN peaks are also apparent, observed in a greater extent than those of SiC_p. Some research [7] classified that AlN is desirable for densification, while some [8] identified the role of AlN as detrimental. Precipitates such as Al_2Cu and congruent Mg_2Si were found both in the as-sintered and age-hardened conditions. Sufficient Mg content of 1.11 wt.% allows congruent Mg_2Si to be formed, which is believed to be beneficial for additional hardening of the composites aside from that of Al_2Cu as the main precipitate phase. Al_2O_3 and Si peaks were also detected in a comparatively lesser extent than other phases' peaks.

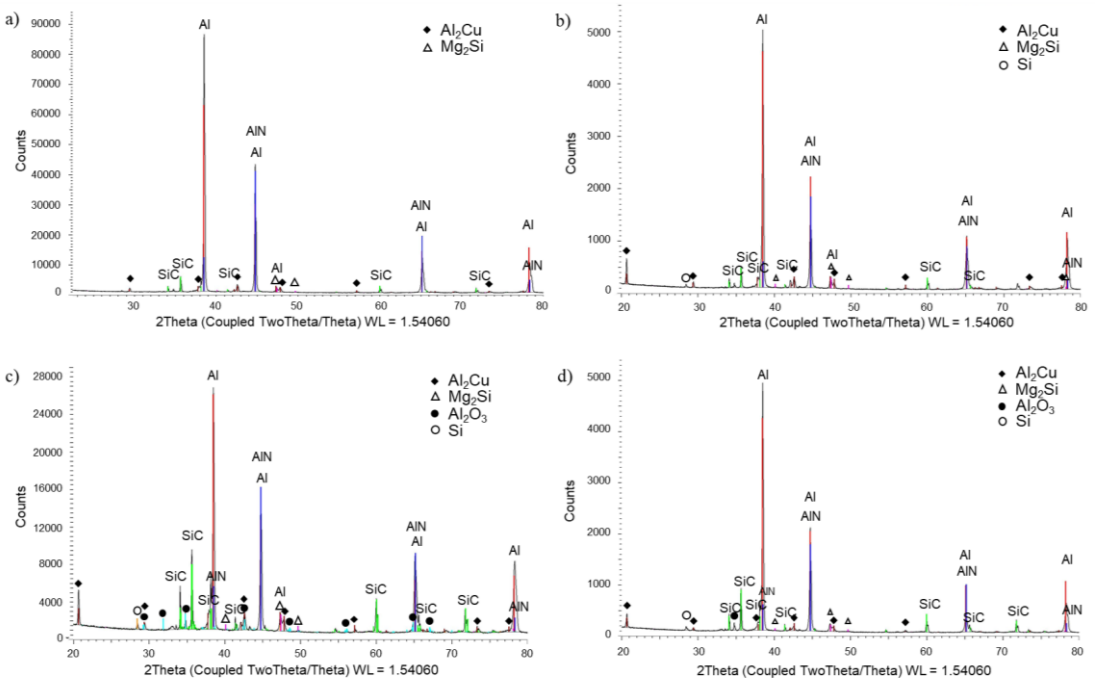

Figure 3. XRD analyses of 10 vol.% SiC_p reinforced aluminium composites in a) as-sintered, b) age-hardened conditions, and 20 vol.% SiC_p reinforced aluminium composites in c) as-sintered, d) age-hardened conditions.

3.1.4 SEM and EDS Analysis

Microstructure investigation at higher magnifications by a secondary mode electron microscopy shows a reasonably good interface between SiC_p and aluminium matrix in the case of 10 vol.% SiC_p addition. However, as mentioned previously, SiC_p clusters are routinely observed when the SiC_p increases to 20 vol.%, as illustrated in Fig. 4 a). This resulted in interparticle or gap porosity accompanying with SiC_p clusters. Figure 4 b) locates EDS analyses at 5 different locations, which confirm the existence of phases found in the as-sintered condition as detailed by EDS peaks of particular elements in Figs. 4 c)-g) for spectrums 1-5 respectively. Spectrum 1 indicates a composition related to that of the aluminium alloy matrix, giving 91.86 wt.% for Al and 5.16 wt.% for Cu, with small amount of 2.98 wt.% O, as listed in the composition table. Spectrum 2 shows a eutectic composition in relevant to its morphology seen on the SEM micrograph. SiC_p was clearly detected in spectrum 3. The Al_2Cu is identified as precipitate in spectrum 5, giving the composition of 45.04 and 54.96 wt.% for Al and Cu respectively. Secondary mode micrograph of the age-hardened composite shows a similar result to that of as-sintered condition as displayed in Fig. 5 a). Five different locations

for EDS analyses are exhibited in Fig. 5 b) where relevant EDS peaks are illustrated in Fig. 5 c)-g) for spectrums 1-5 respectively. The analysed composition of 5 different locations is inclusively summarized within. Spectrum 1 clearly indicates composition of SiC_p while eutectic composition reflects in composition analysed for spectrum 2. The matrix composition is detected as 96.74 wt.% Al and 3.26 wt.% Cu in Spectrum 3 while EDS analysed in spectrum 4 as a mixed composition of mainly Cu, Al and C. Spectrum 5 evidently shows a composition of Al_2Cu precipitate. Such EDS analyses on existing phases are in good agreement with XRD and XRF analyses previously mentioned, with an exception for AlN, which cannot be resolved by SEM used in this current research. Future work is then required to identify such a significant phase.

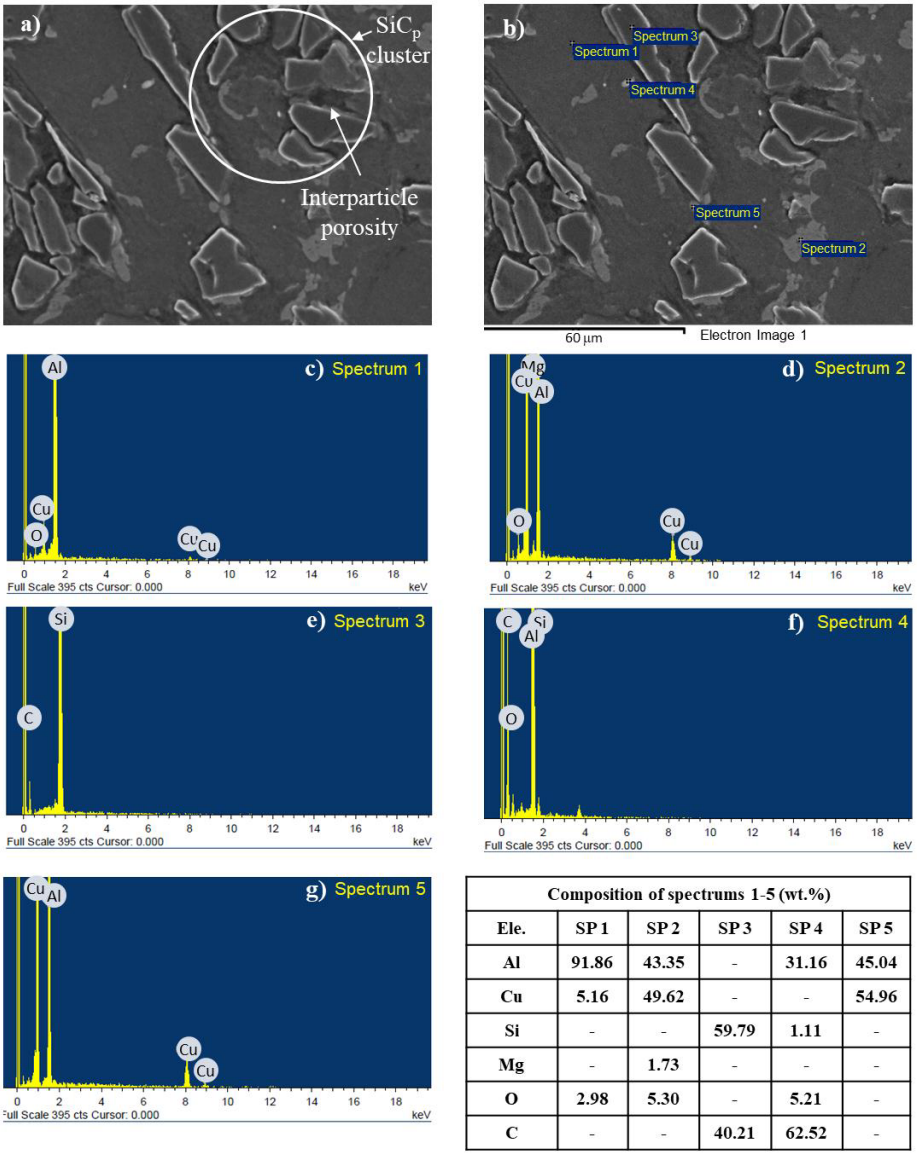

Composition of spectrums 1-5 (wt.%)					
Ele.	SP 1	SP 2	SP 3	SP 4	SP 5
Al	91.86	43.35	-	31.16	45.04
Cu	5.16	49.62	-	-	54.96
Si	-	-	59.79	1.11	-
Mg	-	1.73	-	-	-
O	2.98	5.30	-	5.21	-
C	-	-	40.21	62.52	-

Figure 4. SEM and EDS analysis of as-sintered 20 vol.% SiC_p reinforced aluminium composites.

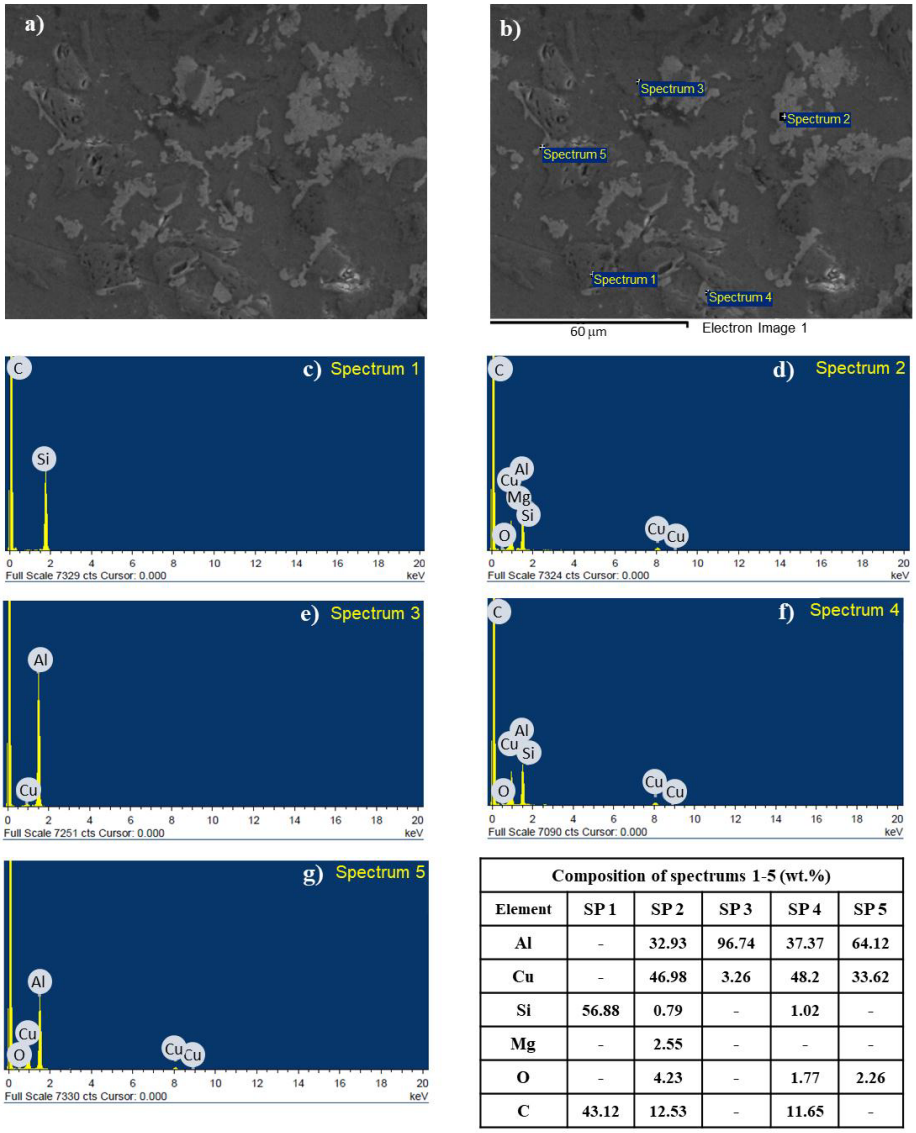

Composition of spectrums 1-5 (wt.%)					
Element	**SP 1**	**SP 2**	**SP 3**	**SP 4**	**SP 5**
Al	-	32.93	96.74	37.37	64.12
Cu	-	46.98	3.26	48.2	33.62
Si	56.88	0.79	-	1.02	-
Mg	-	2.55	-	-	-
O	-	4.23	-	1.77	2.26
C	43.12	12.53	-	11.65	-

Figure 5. SEM and EDS analysis of age-hardened 20 vol.% SiC_p reinforced aluminium composites.

3.2 % Shrinkage and Bulk Density

Percentage of shrinkage in thickness, length and width are listed in Table 2, giving the % volumetric shrinkage likewise. It is seen that % linear shrinkages are rather large, which are in a range of 9.88 - 21.95%. Increasing SiC_p content scales down the % shrinkage, owing to its high thermal stability. Further, by assuming a simple calculation of linear shrinkage (Y_s) as expressed in equation (1) [9] as a function of solid loading of the feedstock (ϕ), theoretical density of the mixed Al powder and SiC_p (ρ_{th}) according to equation (2), and the final sintered density (ρ), the Y_s can be obtained as summarized in Table 2. It is noted that the calculated linear shrinkage is significantly smaller than the measured ones. The volumetric shrinkage is essentially high, due to high amount of binder used at 45 vol.% plus densification by liquid-phase sintering involved. Increasing SiC_p content from 10 to 20 vol.% therefore results in a significant reduction in the volumetric shrinkage from 46.62% to 34.54%.

$$Y_s = 1 - \{\phi/(\rho/\rho_{th})\}^{1/3} \quad (1)$$

Table 3 summarises green and sintered densities of the composites, giving the optimum sintered density of 2.63 g/cm^3 for 10 vol.% SiC_p-reinforced aluminium composite. This accounts for 93.1% theoretical sintered density according to the rule of mixture. Equations (2) and (3) express theoretical density for the green compact ($\rho_{green,\,th}$) and sintered sample ($\rho_{sinter,\,th}$) respectively.

$$\rho_{green,\,th} = \rho_{Al}V_{Al} + \rho_{SiC}V_{SiC} + \rho_{binder}V_{binder} \quad (2)$$

$$\rho_{sinter,\,th} = \rho_{Al}V_{Al} + \rho_{SiC}V_{SiC} \quad (3)$$

where ρ_{Al}, ρ_{SiC}, and ρ_{binder} are densities of aluminium alloy (2.78 g/cm^3) [10], SiC (3.20 g/cm^3) and multi-component binder (0.94 g/cm^3). Accordingly, V_{Al}, V_{SiC} and V_{binder} are volume fractions of aluminium alloy, SiC_p and multi-component binder respectively, where $V_{Al} + V_{SiC} + V_{binder} = 1$ for equation (2) and $V_{Al} + V_{SiC} = 1$ for equation (3). Increasing SiC_p content therefore deteriorates the sintered density, due possibly to agglomeration behaviour of high surface energy SiC_p [11, 12] during feedstock preparation. These SiC_p clusters and interparticle porosity still remained even after the samples experiencing the liquid phase sintering.

Table 2. % Average shrinkage in thickness, length, width, and volume.

SiC_p (vol.%)	% Shrinkage				% Calculated linear shrinkage (Y_s)
	Thickness	Length	Width	Volume	
10	21.95	17.63	16.99	46.62	16.12
20	9.88	15.18	14.47	34.54	13.45

Table 3. Average green and sintered density, and macro hardness properties.

SiC_p (vol.%)	Bulk green density (g/cm^3)		Bulk sintered density (g/cm^3)		Macro Vickers hardness, (H_v)	
	Measured	%Theoretical	Measured	%Theoretical	As-sintered	Age-hardened
10	1.83	93.37	2.63	93.1	132.6	160.8
20	1.84	92.93	2.43	85.0	125.0	164.2

3.3 Macro Vickers Hardness

Macro Vickers hardness result shows increased values after age-hardening for both composites with 10 and 20 vol.% SiC_p additions. The maximum macro hardness value was measured at 164.2 H_v for 20 vol.% SiC_p - aluminium composite after age-hardening, as listed in Table 3. The precipitation of fine Al_2Cu and Mg_2Si during age-hardening are possibly the cause of hardening effect.

4 Discussion

4.1 Densification of the PIMed SiC_p-Reinforced Aluminium Composites

As previously shown that the calculated linear shrinkage of the PIMed composite is 13.45-16.12%. However, the measured linear shrinkage of the composites is rather high, essentially for the

volumetric shrinkage (34.54-46.62%), which is related to high binder content and liquid phase sintering involved. If the shrinkage related to eliminating of the binder is excluded, effect of the remaining solid phases, i.e., aluminium and SiC_p on shrinkage is now considered. After the binder was rid of, the sample then entered the liquid phase sintering. Additional shrinkage is due mainly to aluminium powder, which partly melted to facilitate particle rearrangement, and then shrank upon solidification. In this current research work, densification occurred without any significant warpage or dimension instability fortunately. Comparative work of previous research [11] investigated sintering of 20 vol.% SiC_p-reinforced aluminium composite, sintered at a higher temperature of 740^oC over 1 hour reported the density of 2.52 g/cm^3 and hardness of 95.9 and 136.9 H_v in the as-sintered and age-hardened conditions respectively without any warpage. By replacing the aluminium powder with one of a smaller size (39.6 μm), a greater degree of densification prevailed, due to shorter diffusion distance and larger curvature stresses [12]. Though, gaps between SiC_p-SiC_p and SiC_p-Al interfaces were sealed in this case, dimension stability is nevertheless sacrificed. Therefore, in this current work, the sintering scheme has been changed by lowering sintering temperature 650-660 ^oC. Extending the sintering period is then obligatory to attain effective sinterability of the composite, offering relatively greater hardness values of 125.0 and 164.2 H_v in the as-sintered and age-hardened conditions as mentioned previously. Lower sintering temperature is to avoid dimension instability and extended sintering time is to aid diffusion process to take place when the sintering temperature is approaching the melting temperature.

As the liquid phase sintering proceeded, higher diffusion rate allowed [12] 1) rearrangement of aluminium powder and SiC_p favourable for particle packing, 2) solution-precipitation suitable for pore filling and through the 3) final stage of densification. In the early stage of liquid phase sintering of this type of composite, as the aluminium oxide skin was consumed [13], Mg played a key role on wetting of the liquid aluminium on the surface treated SiC_p. [14]. Spreading of the liquid phase then dissolved the sintered bonds and rearranged the aluminium powder and SiC_p by providing capillary force to pulls all solid grains together [12]. Except for the SiC_p, the aluminium powder is of course easily soluble in the liquid melt, which enhanced the transport rate, resulting in grain coarsening and densification. Further, pore isolation and annihilation is associated with reduction of surface energy in this final stage. Reasonably good sintered density of 2.63 g/cm^3 at 93.1% theoretical is then achieved for 10 vol.% SiC_p reinforced aluminium composite. Nevertheless, increasing SiC_p content from 10 to 20 vol.% slowed down the mass transport due to its lower solubility in the liquid melt. More effort was then required to pull more solid grains of SiC_p and the remaining aluminium powder and, resulting in less % shrinkage and inferior densification.

4.2 Hardening of the PIMed SiC_p-Reinforced Aluminium Composites

To consider hardening mechanisms in the PIMed SiC_p-Reinforced Aluminium Composites, roles of SiC_p addition and age-hardening are now discussed. First, hard and abrasive SiC_p of a finer size was used to reinforce aluminium-copper alloy. Its intrinsic hard-abrasive property rendered the increment in macro hardness as the hardness indention stretching over an area accounting for hundreds of SiC_p. The influence of interparticle porosity existing in the SiC_p clusters found in the 20 vol.% SiC_p addition is then retarded, though this interparticle porosity reflects the inferior sintered density as mentioned earlier in section 3.2. However, previous work [15] has reported exceeding amount of SiC_p addition up to 30-40 vol.% has proof to give deleterious density and hardness.

Secondly, roles of precipitates such as AlN, Al_2Cu and Mg_2Si are considered. Though, AlN peaks are quite evident from the XRD results, confirmation by SEM and EDS is still an issue in this current work. It was reported elsewhere [16, 17] on sub-micron sizes of AlN found in aluminium composite produced by a liquid-route process at 900-1000 ^oC. However, in the solid-route process of powder metallurgy [18], it was also documented that AlN shell was formed enveloping the pure aluminium powder by nitridation at 560 ^oC for 6-18 h in N_2 flow prior to sintering. TEM characterization of this AlN shell revealed an aluminium matrix with a large number of AlN nanoparticles in a 10-50 nm. Therefore, it might be presumed that the AlN formation is possible over the 650-660 ^oC sintering

temperature in this current work. However, due to the shorter exposure time to N_2, AlN might be formed as a thin-shell structure surrounding such aluminium powder and make it difficult to recognize. Further work is then required to identify morphology and preferential sites of AlN in order to explain its function on the strengthening effect of the composite. In addition, the formations of Al_2Cu and Mg_2Si are confirmed by both XRD and EDS point analysis results. Though, peaks of Al_2Cu and Mg_2Si were also detected both in the as-sintered and after age-hardening, the latter is theoretically fine and coherent. These fine coherent precipitates formed after age-hardening offer hardness increment in a range of 23.5 - 31.4%.

5 Conclusions

According to the experimental results, it can be concluded that the PIMed aluminium composites reinforced with 10 -20 vol.% SiC_p provided uniform microstructure, giving reasonably good sintered density of 93.1% theoretical at 2.63 g/cm^3 and maximum macro Vickers hardness of 164.2 H_v after age-hardening. Densification and high values of linear and volumetric shrinkage are due to liquid phase sintering. Hardening is influenced by SiC_p addition and the roles of AlN, Al_2Cu and Mg_2Si precipitates.

References

1. S. Rawal, JOM **53** 14-17 (2001)
2. C. Yan, W. Lifeng, R. Jianyue, Chin. J. Astron. **21** 578-584 (2008)
3. M. Dyzia, Materials, **11** 1-13 (2018)
4. S.-J. L., Kang, *Sintering: densification, grain growth & microstructure* (2005)
5. R. M. German, *Sintering: From Empirical Observations to Scientific Principles* (2014)
6. A. Arockiasamy, R. M. German, P. Wang, M. F. Horstemeyer, W. Morgan, S. J. Park Sintering, Powder. Metall. **54** 354-359 (2011)
7. T. W. Kim, Mater. Sci. Eng., A **483-484** 648-651 (2008)
8. I. A. MacAskill, R. L. Hexemer Jr, I. W. Donaldson, D. P. Bishop, J. Mater. Process. Technol. **210** 2252-2260 (2010)
9. D. F. Heaney, *Handbook of Metal Injection Molding* (2012)
10. J. M. Martín, F. Castro, J. Mater. Process. Technol. **143-144** 814-821 (2003)
11. A. Ngeekoh, V. Thongnoppakoon, A. Changlor, T. Jindangam, N. Phongreed, T. Patcharawit, N. Chuankrerkkul, the 41st Cong. Sci. and Tech. of Thai. (2014)
12. R. M. German, P. Suri, S. J. Park, J. Mater. Sci. **44** 1-39 (2009)
13. A. Kimura, M. Shibata, M. Katayama, T. Kanie, H. Takada, Appl. Phys. Lett. **70** 3615-3617 (1997)
14. J. Hashim, L, Looney, M. S. J. Hashmi, J. Mater. Process. Technol. **119** 324-328 (2001)
15. T. Patcharawit, P. Tongkhon, A. Wiangsamut, P. Auisungnoen, N. Chuankrerkkul, Appl. Mech. Mater. **376** 17-22 (2013)
16. C. Borgonovo, D. Apelian, M. M. Makhlouf, JOM **63** 57-64 (2014)
17. S. Kumari, U. Pillai, and B.C. Pai, J. Alloys Compd. **509** 2503-2509 (2011)
18. M. Balog, P. Yu, M. Qian, M. Behulova, P. Svec Sr, R. Cicka, Mater. Sci. Eng., A **562** 190-195 (2013)